frontiers in Earth Science

ORIGINAL RESEARCH
published: 01 July 2021
doi: 10.3389/feart.2021.687382

Seismic Reflection Images of Possible Mantle-Fluid Conduits and Basal Erosion in the 2011 Tohoku Earthquake Rupture Area

Jin-Oh Park[1], Tetsuro Tsuru[2], Gou Fujie[3], Ehsan Jamali Hondori[1], Takanori Kagoshima[4], Naoto Takahata[1], Dapeng Zhao[5] and Yuji Sano[6]*

[1]Atmosphere and Ocean Research Institute, University of Tokyo, Kashiwa, Japan, [2]Department of Marine Resources and Energy, Tokyo University of Marine Science and Technology, Tokyo, Japan, [3]Japan Agency for Marine–Earth Science and Technology, Yokohama, Japan, [4]Department of Environmental Biology and Chemistry, University of Toyama, Toyama, Japan, [5]Department of Geophysics, Graduate School of Science, Tohoku University, Sendai, Japan, [6]Center for Advanced Marine Core Research, Kochi University, Nankoku, Japan

OPEN ACCESS

Edited by:
Sara Martinez-Loriente, Instituto de Ciencias del Mar (CSIC), Spain

Reviewed by:
Masanao Shinohara, The University of Tokyo, Japan
Manel Prada, Instituto de Ciencias del Mar (CSIC), Spain

***Correspondence:**
Jin-Oh Park
jopark@aori.u-tokyo.ac.jp

Specialty section:
This article was submitted to Structural Geology and Tectonics, a section of the journal Frontiers in Earth Science

Received: *29 March 2021*
Accepted: *17 June 2021*
Published: *01 July 2021*

Citation:
Park J-O, Tsuru T, Fujie G, Jamali Hondori E, Kagoshima T, Takahata N, Zhao D and Sano Y (2021) Seismic Reflection Images of Possible Mantle-Fluid Conduits and Basal Erosion in the 2011 Tohoku Earthquake Rupture Area. Front. Earth Sci. 9:687382. doi: 10.3389/feart.2021.687382

Multi-channel seismic reflection and sub-bottom profiling data reveal landward-dipping normal faults as potential conduits for mantle-derived fluids in the coseismic slip area of the 2011 Tohoku earthquake (M_w9.0). Normal faults below the helium isotope anomaly sites appear to develop through the forearc crust (i.e., the seafloor sedimentary section and Cretaceous basement) and to evolve to lower dip angles as extension progresses deeper, potentially extending down to the mantle wedge, despite their intermittently continuous reflections. The faults are characterized by high-amplitude, reverse-polarity reflections within the Cretaceous basement. Moreover, deep extension of the faults connecting to a low-velocity region spreading from the Cretaceous basement into the mantle wedge across the forearc Moho suggests that the faults are overpressured by local filling with mantle-derived fluids. The locations of the normal faults are roughly consistent with aftershocks of the 2011 Tohoku earthquake, which show normal-faulting focal mechanisms. The 2011 Tohoku mainshock and subsequent aftershocks can lead the pre-existing normal faults to be reactive and more permeable so that locally trapped mantle fluids can migrate up to the seafloor through fault fracture zones. The reactivated normal faults may be an indicator of shallow coseismic slip to the trench. Locally elevated fluid pressures can decrease the effective normal stress for the fault plane, facilitating easier slip along the fault and local tsunami. The landward-dipping normal faults developing from the seafloor down into the Cretaceous basement are predominant in the middle slope region of the forearc. A possible shear zone with high-amplitude, reverse-polarity reflections above the plate interface, which is almost localized to the middle slope region, suggests more intense basal erosion of the overlying plate in that region.

Keywords: fluid migration, seismic reflection, normal fault, shallow coseismic slip, basal erosion

INTRODUCTION

Large megathrust earthquakes along subduction zones pose seismic and tsunami threats to densely populated coastal cities. Many megathrust earthquakes and tsunamis have occurred in the Japan Trench margin (**Figure 1**) where the Pacific plate subducts beneath the northeast Japan arc (i.e., the Okhotsk plate) at a convergence rate of 8.6 cm/yr (DeMets et al., 1990; Yamanaka and Kikuchi, 2004). The forearc region of the Japan Trench margin is typically characterized by extensional subsidence and normal faults associated with tectonic or basal erosion (i.e., removal of material from the base of the overlying plate), which results from the subduction of the Pacific plate (von Huene and Lallemand, 1990). Coseismic rupture of the 2011 Tohoku earthquake (M_w9.0) nucleated at a depth of approx. 20 km has propagated along the shallow plate-boundary fault nearly all the way to the trench, yielding powerful tsunami waves (e.g., Ide et al., 2011; Iinuma et al., 2012). Pore fluid pressure along the plate interface (i.e., plate-boundary fault) might play an important role in the occurrence of large megathrust earthquakes (e.g., El Hariri et al., 2010). Helium isotopes are useful for elucidating fluid behavior. They might provide crucially important information about the source of interplate fluids. Geochemical evidence points to a sharp increase in mantle-derived helium in bottom seawater near the rupture zone 1 month after the 2011 Tohoku earthquake (Sano et al., 2014). Taking account of the locations (sites N3, N2, N1, and R in **Figure 1**) of helium isotope anomaly, mantle-derived fluids are believed to have migrated from the mantle wedge up to the forearc seafloor through the normal faults. However, the geometry and characteristics of the normal faults as fluid conduits remain poorly understood despite many earlier seismic reflection studies (e.g. Kodaira et al., 2017; Tsuru et al., 2000;

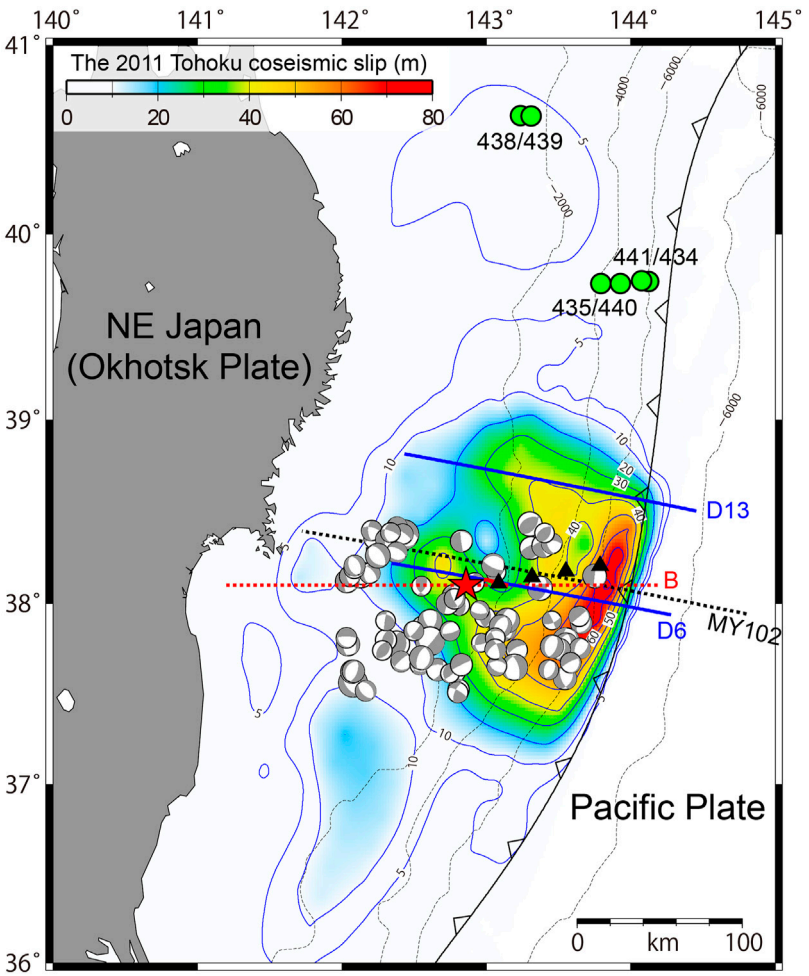

FIGURE 1 | Bathymetry map of the Japan Trench margin off northeast Japan. The Pacific plate subducts beneath the Okhotsk plate (northeast Japan) at a convergence rate of 8.6 cm/yr (DeMets et al., 1990). Heavy blue, black dotted, and red dotted lines respectively mark MCS lines D6 and D13 (this study), OBS line MY102 (Miura et al., 2005), and seismic tomography line B (Liu and Zhao, 2018). Four black triangles mark helium isotope anomaly sites (Sano et al., 2014): sites N3, N2, N1, and R from west to east. The 2011 Tohoku (M_w9.0) coseismic slip model with colors and thin blue contours is given by Iinuma et al. (2012). The red star denotes the mainshock epicenter of the 2011 Tohoku earthquake. Centroid moment tensors (CMTs) for aftershocks of the 2011 Tohoku event within the overlying Okhotsk plate (Asano et al., 2011) are displayed around the MCS and OBS lines. Green circles show DSDP site numbers of 434–441 (Nasu et al., 1980).

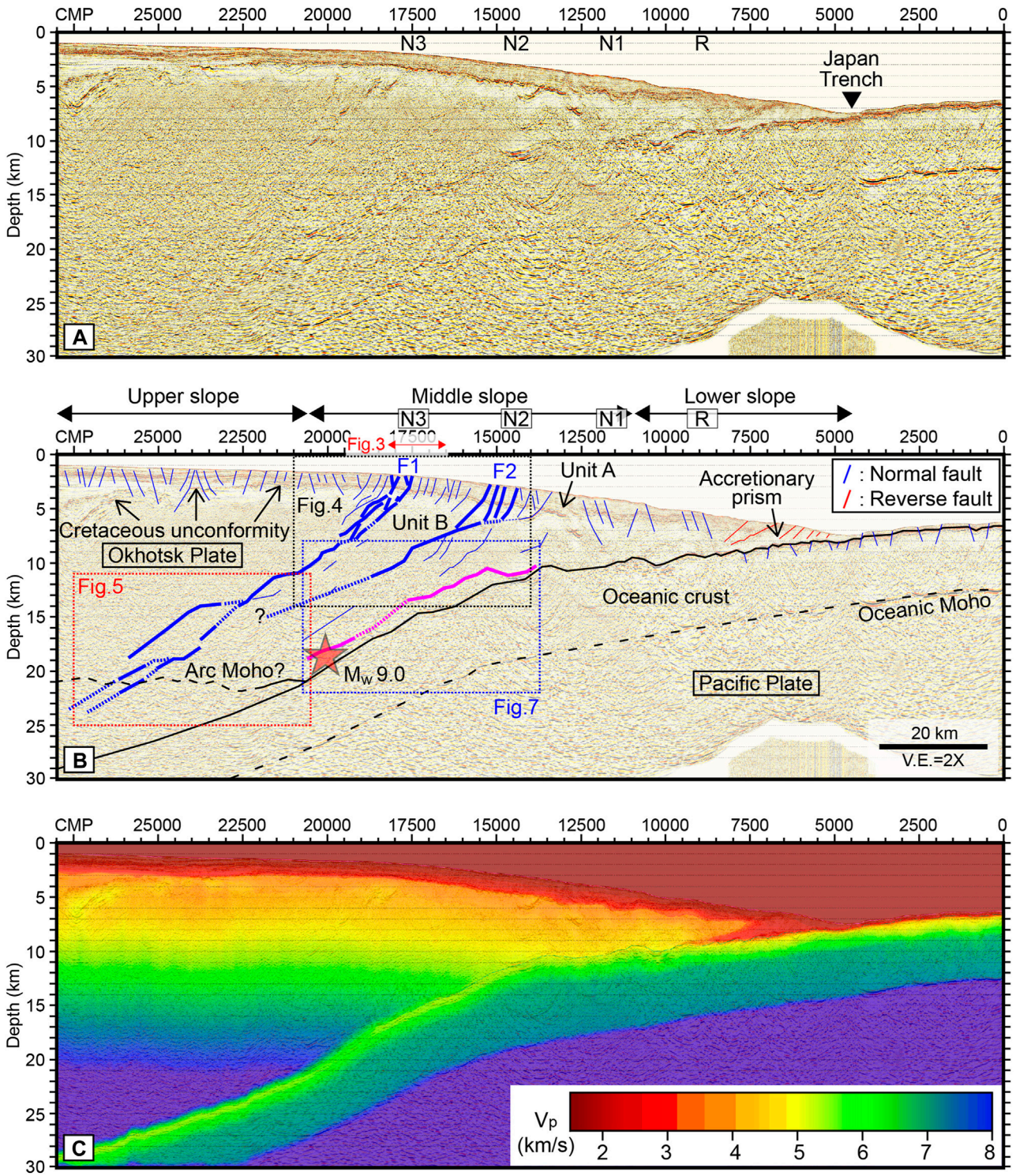

FIGURE 2 | Pre-stack depth migrated (PSDM) seismic profile, interpretation, and V_p model for the PSDM on line D6. **(A)** Uninterpreted PSDM profile. Locations of the helium isotope anomaly sites (Sano et al., 2014) are displayed: N3, N2, N1, and R. **(B)** Interpreted PSDM profile. The red star marks the hypocenter of the 2011 Tohoku mainshock (M_w9.0). Normal and reverse faults are denoted respectively by thin blue and red lines. A thin red line below site N3 in the middle slope region marks the SBP line depicted in **Figure 3**. It is noteworthy that landward-dipping normal faults (thick blue F1 and F2 below sites N3 and N2, respectively) and a potential shear zone (thick pink) develop in the middle slope region. Thin black, red, and blue dotted boxes are enlarged respectively in **Figure 4**, **Figure 5**, and **Figure 7**. **(C)** V_p model overlaid by the PSDM profile.

Tsuru et al., 2002; von Huene et al., 1994). Moreover, structural features related to basal erosion causing the normal faulting are less documented.

As described herein, we present seismic reflection images of large-scale normal faults as mantle-fluid conduits potentially across the entire forearc crust and a shear zone associated with basal erosion in the coseismic slip region of the 2011 Tohoku earthquake. Furthermore, we discuss fluid migration processes along normal faults, implications of normal faults for shallow coseismic slip, and basal erosion in the forearc crust of the Japan Trench margin.

SEISMIC REFLECTION DATA AND INTERPRETATION

Multi-channel seismic (MCS) reflection data on approximately 175-km-long line D6 (**Figure 1**) were acquired by R/V *Kairei* of the Japan Agency for Marine–Earth Science and Technology (JAMSTEC) in May 2011, immediately after the Tohoku earthquake (M_w9.0). For deep-penetration seismic imaging, a large air-gun array (total volume approx. 128 L) was used as the controlled sound source. The MCS data were collected with a 50 m shot interval and were recorded with an approx. 6,000 m, 444-channel streamer with 12.5 m group spacing. We applied conventional MCS data processing techniques including trace editing, band-pass filtering, spherical divergence correction, signature deconvolution, multiple suppression by parabolic radon transforms, and common midpoint (CMP) sorting to obtain pre-conditioned CMP gathers for which the relative amplitudes are preserved. Using the CMP gathers, we developed P-wave interval velocity models with a layer stripping method and Kirchhoff pre-stack depth migration (PSDM) velocity analysis (Yilmaz, 2001). Velocity data from ocean-bottom seismograph (OBS) wide-angle seismic refection and refraction survey (Miura et al., 2005) on line MY102 (**Figure 1**) guided the PSDM velocity model building. We performed grid-based traveltime tomography to refine the PSDM velocity model. Both the final PSDM profile and P-wave interval velocity model are shown in **Figure 2** and **Supplementary Figure S1**. To support the quality of the migration at depth, we present PSDM gathers and their semblance plots at several CMPs (**Supplementary Figure S1**). Additionally, we have conducted 3.5 kHz sub-bottom profiling (SBP) during the R/V *Shinsei-maru* cruise (KS-16-17) in November 2016 to obtain high-resolution seismic images on sites of a helium isotope anomaly that was reported by Sano et al. (2014).

General Interpretation

On the PSDM profile of line D6 (**Figures 2A,B**), we observe a bright reflector at the topmost oceanic crust (i.e., plate interface) of the Pacific plate subducting beneath the overlying Okhotsk plate, which can be traceable to more than 100 km landward from the Japan Trench axis and down to approx. 21 km depth from the sea surface. The seaward Pacific plate is characterized by many horst and graben structures with normal faults. A strong reflector of oceanic Moho discontinuity, which is observed beneath the oceanic crust before subduction, is also observed even after subduction of the Pacific plate, up to more than 100 km landward from the Japan Trench axis. We identify prominent reflections located at a maximum of approx. 2 km above the plate interface from the CMP 14000 to 20500, which might be interpreted as a shear-zone associated with plate subduction (**Figure 2B**).

The seafloor morphology suggests that the overlying plate is divisible into three domains from west to east: upper, middle, and lower slope regions. **Figure 1** shows that the plate interface in the upper to lower slope regions on the PSDM profile of line D6 was ruptured completely during the 2011 Tohoku event (e.g., Iinuma et al., 2012). Based on seismic reflection characteristics and Deep Sea Drilling Project (DSDP) drilling results (Nasu et al., 1980), the overlying plate is divided simply into two seismic units (e.g., Kimura et al., 2012; Tsuru et al., 2000; von Huene et al., 1994) from top to bottom: Unit A of Recent to Miocene sediments overlies Unit B of the Cretaceous basement (**Figure 2B**). A bright reflector between Units A and B is interpreted as an erosional unconformity distinguishing the Miocene sediments from the Cretaceous basement. The Pleistocene accretionary prism, composed mainly of pelagic sediments that were conveyed from subducting Pacific plate, is localized immediately landward of the Japan Trench. Whereas many normal faults develop in the upper and middle slope regions, reverse faults are localized in the lower slope region. A mantle wedge is identified in the upper slope region. We observe a reflector with low amplitude of arc Moho landward from CDP 21000 at approx. 21 km depth. Its location is guided by P-wave velocity (V_p) models from ocean bottom seismograph (OBS) survey on line MY102 (Miura et al., 2005) (**Figure 1**). Similar arc Moho reflection is observed at approx. 21 km depth on another PSDM profile of line D13 (**Figure 1** and **Supplementary Figure S2**) which is about 65 km north away from line D6.

Normal Faults Below Mantle Helium Anomaly Sites

On the high-resolution SBP profile (**Figure 3**) close to mantle helium isotope anomaly site N3 (Sano et al., 2014) around CMP 17500 on the MCS line D6 (**Figure 2B**), one can observe a subsidence structure in the hanging wall of the landward-dipping normal fault "F1." A well-stratified sedimentary sequence below the seafloor is clearly cut by normal fault F1, suggesting that the fault remains active. The PSDM profile of line D6 supports investigation of the deep extension of the normal fault F1. **Figure 2B** and **Figure 4** show that it cuts the top of the Cretaceous basement (Unit B) as well as the overlying Recent to Miocene sedimentary layer (Unit A). Normal fault F1 with an approx. 50° dip within the sedimentary layer (Unit A) appears to evolve to lower dip angles within the Cretaceous basement (Unit B) as extension progresses deeper (i.e, approx. 20° dip at ~10 km depth and approx. 17° dip at ~20 km depth), eventually down to the mantle wedge at approx. 21 km depth. The approx. 70-km-long normal fault F1 exhibits fault offsets of approx. 50 m averaged over the entire sedimentary section (approx. 1.2 km

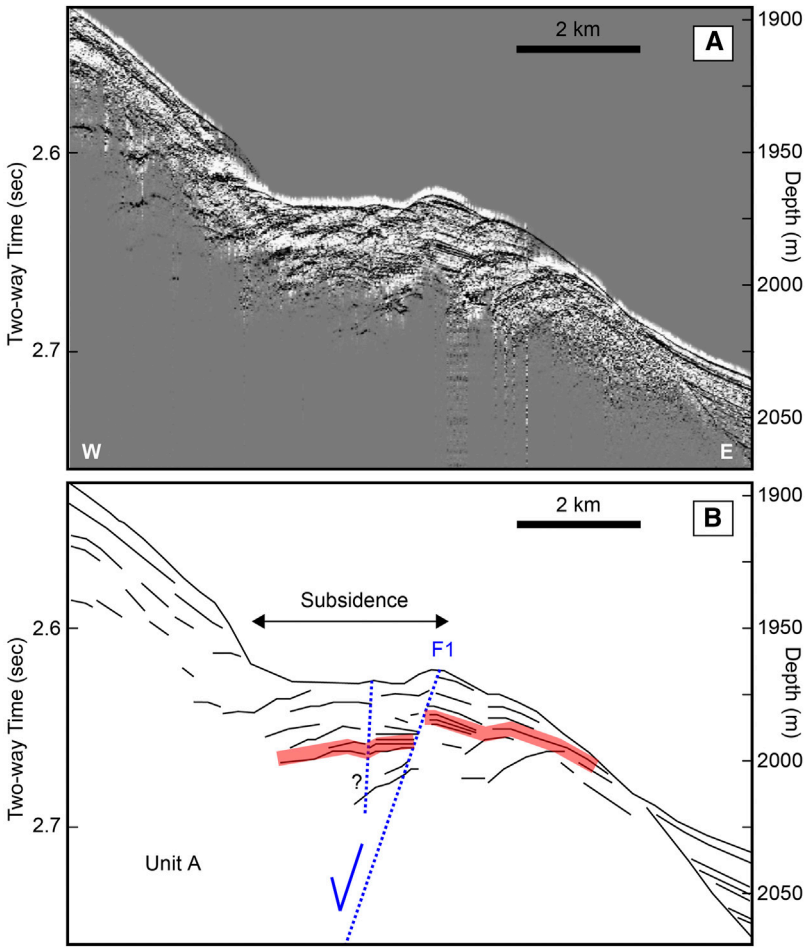

FIGURE 3 | High-resolution SBP profile and interpretation around site N3. Location of the SBP profile (~11 km long) is presented in **Figure 2B**. **(A)** Uninterpreted SBP profile. **(B)** Interpreted SBP profile. Heavy blue dotted line marks a landward-dipping normal fault (F1). It is noteworthy that displacement of a stratified sedimentary sequence (in red) below the seafloor and subsidence structure in the hanging wall block, which are caused by normal faulting.

thick) and approx. 200 m at the top of the Cretaceous basement (**Figure 4** and **Supplementary Figure S3A**), implying that normal faulting has been reactivated many times and that it remains active. Fault F1 is also identified on another PSDM profile of line D13 (**Supplementary Figure S2**).

Normal fault F1 shows high-amplitude, reverse-polarity reflections at depths of ~5, ~7, ~10, ~12, and ~20 km (**Figure 4** and **Figure 5**), which are caused by a decrease in acoustic impedance (velocity × density) across the fracture zone of the fault, apparently indicating a fluid-rich and consequently overpressured section along the fault. In fact, fluid pressures influence the effective stress state acting on the fault zone (e.g., Hubbert and Rubey, 1959). An increase in fluid pressure, because of hydrofracture or dilation within the fault zone, would cause decreases in effective stress and V_p, and therefore, a subsequent reversal of acoustic impedance across the fault (e.g., Tobin et al., 1994), resulting in the reverse-polarity reflection. The deep portion of fault F1 from approx. 12 km down to approx. 22 km depth is spatially correlated with a low V_p zone from seismic tomography (Liu and Zhao, 2018) on line B (**Figure 1** and **Figure 6**) using suboceanic earthquakes. The low V_p zone suggests that the fault fracture zone is potentially filled with fluids, although it cannot be verified from PSDM velocities derived from near-vertical MCS data. Considering the geometry by which the low V_p zone extends into Unit B from the mantle wedge and includes the deep portion of fault F1, we infer that mantle-derived helium at site N3 originated from the mantle wedge and migrated through fault F1, eventually reaching the seafloor at site N3. The mantle wedge fluids might result from dehydration reactions of the subducting Pacific slab (Zhao et al., 2015).

We observe another landward-dipping normal fault "F2" below mantle helium anomaly site N2 (Sano et al., 2014) around CMP 14500 on the MCS line D6 (**Figure 2B** and **Figure 4**). Normal fault F2 cuts the top of the Cretaceous basement (Unit B) as well as the overlying Recent to Miocene sedimentary layer (Unit A). Normal fault F2 with an approx. 52° dip within the sedimentary layer (Unit A) appears to evolve to a lower dip angle of approx. 12° dip at approx. 8 km depth within the

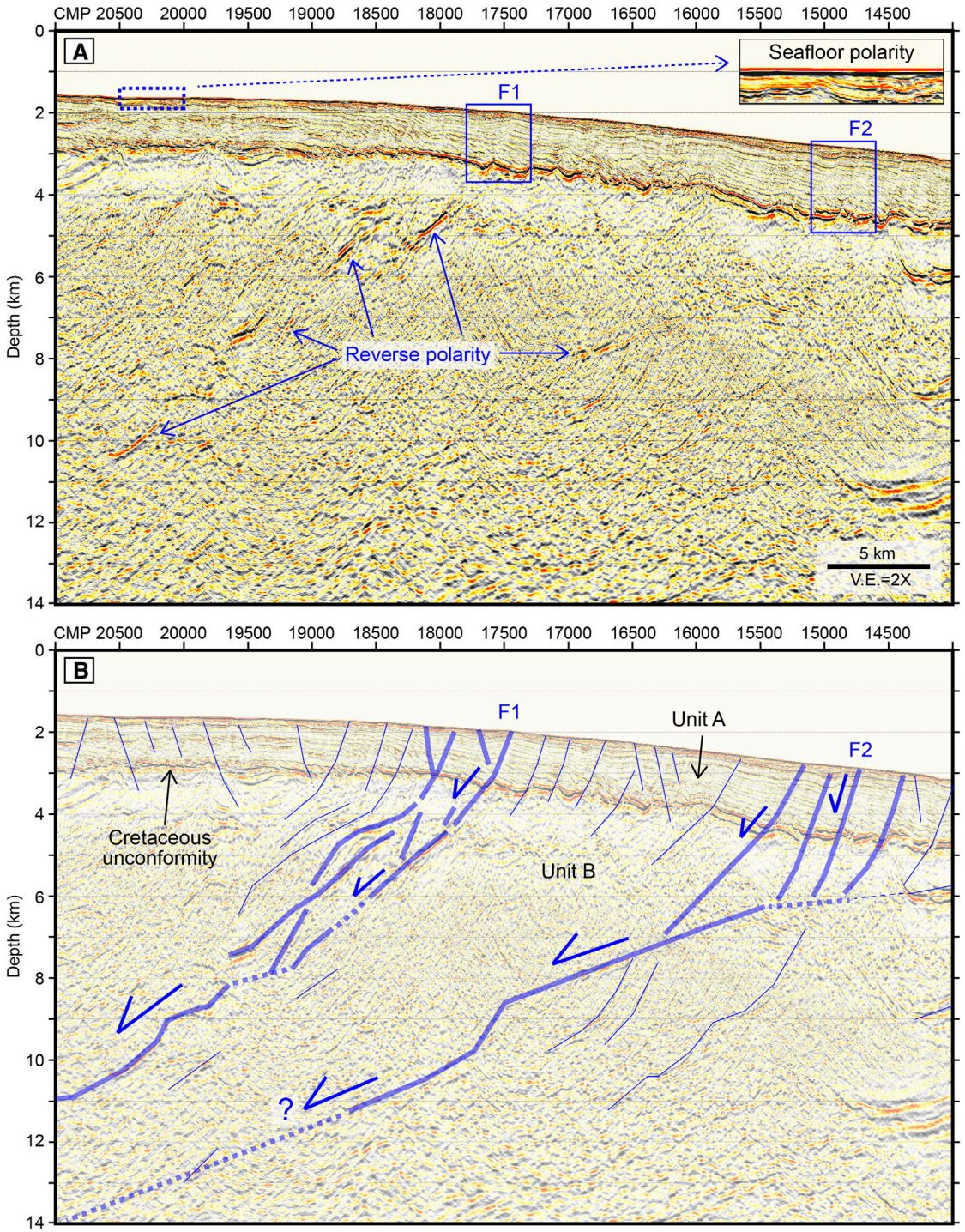

FIGURE 4 | Enlarged PSDM section on line D6 and its interpretation showing landward-dipping normal faults of F1 and F2 in the middle slope region. Location of the section is presented in **Figure 2B**. **(A)** Uninterpreted PSDM section. High-amplitude, reverse-polarity reflections (black–red–black) of the normal faults F1 and F2, compared with seafloor reflection (red–black–red), suggesting high pore pressure of the fault zones. Close-up figures (thin blue boxes) of the faults F1 and F2 at shallow depth are shown in **Supplementary Figures S3A,B**, respectively. **(B)** Interpreted PSDM section. Most normal faults cut down the Cretaceous erosional unconformity.

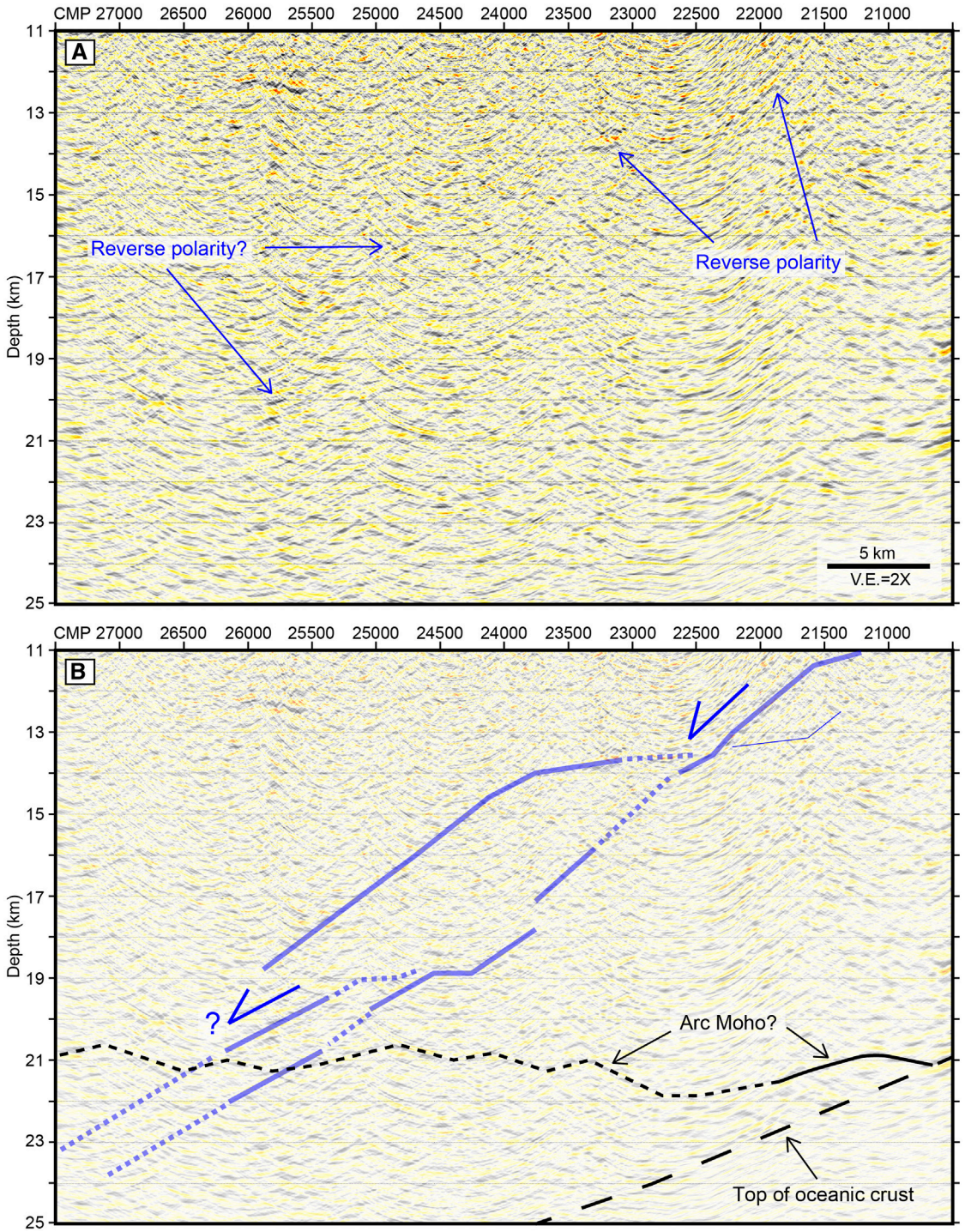

FIGURE 5 | Enlarged PSDM section on line D6 and its interpretation showing deep extension of the landward-dipping normal fault F1 in the middle slope region. The section location is presented in **Figure 2B**. **(A)** Uninterpreted PSDM section. Reverse-polarity reflections (black–red–black) of fault F1. **(B)** Interpreted PSDM section.

Cretaceous basement (Unit B) as extension progresses deeper. Taking into account the geometry fault F2, the depth extension of fault F2 appears to converge into fault F1 at approx. 17 km depth rather than into either the plate interface or the mantle wedge. The approx. 60-km-long normal fault F2 exhibits fault offsets of approx. 30 m averaged over the entire sedimentary section (approx. 1.5 km thick) and approx. 100 m at the top of the Cretaceous basement (**Figure 4** and **Supplementary Figure S3B**), implying that normal faulting has been reactivated many times and that it

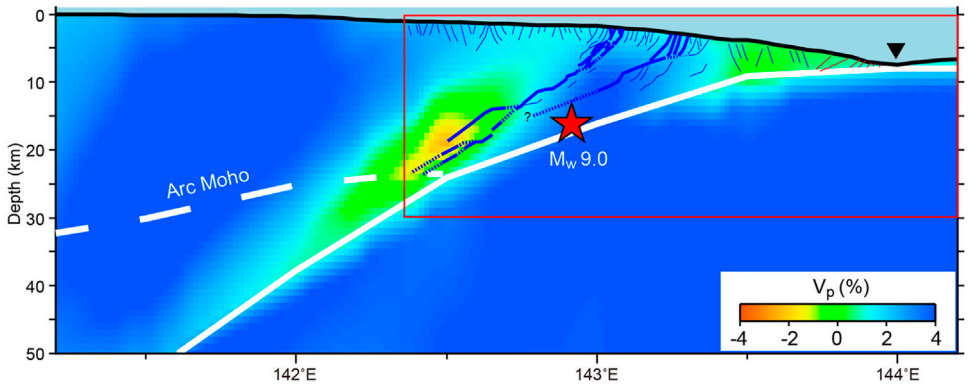

FIGURE 6 | P-wave tomographic image (Liu and Zhao, 2018) along the profile B (**Figure 1**). Fault interpretations (**Figure 2B**) on the PSDM profile of line D6 are shown in red box. The red star marks the hypocenter of the 2011 Tohoku mainshock (M_w9.0).

remains active. Fault F2 is also identified on another PSDM profile of line D13 (**Supplementary Figure S2**).

Similar to fault F1, normal fault F2 shows a high-amplitude, reverse-polarity reflection at approx. 8 km depth (**Figure 4**), suggesting a fluid-rich and therefore overpressured section along the fault. Considering the reverse polarity of both faults, their geometry and the presence of mantel-derived helium at site N2, we interpret that fluids migrate upward from the mantle-wedge through F1 and F2 to the surface. When we project aftershocks of the 2011 Tohoku mainshock (**Figure 1**) on the MCS profile of line D6, many normal-fault-type aftershocks (M_w2 to M_w5) within the overlying plate are widely distributed in the upper and middle slope regions, suggesting reactivations of faults F1 and F2 after the 2011 mainshock.

We also observe several landward-dipping normal faults around mantle-helium anomaly sites N1 and R (Sano et al., 2014), respectively, around CMP 12000 and 9,000 on MCS line D6 (**Figure 2B**). However, we cannot identify deep extensions of faults within Unit B, probably because of insufficient seismic resolution to image the faults or little contrast in acoustic impedance across the deep fault.

DISCUSSION

Fluid Migration Along Active Normal Faults

We identify two landward-dipping normal faults F1 and F2 below the mantle-helium isotope anomaly sites N3 and N2, respectively, which extend into the Cretaceous basement and which potentially reach the mantle wedge. Mantle-derived helium is inferred to ascend through the normal faults as potential fluid conduits, eventually producing mantle helium isotope anomaly near the seafloor (Sano et al., 2014). Significant change of the mantle helium isotope anomaly after the 2011 Tohoku earthquake suggests that faults F1 and F2 are associated with coseismic rupture propagation (e.g., Ide et al., 2011; Iinuma et al., 2012) from the mantle wedge to the near trench and thus the episodic forearc extension during the 2011 Tohoku event. Postseismic wedge-stress relaxation might help normal faults to maintain their activities. Two scenarios can be regarded as explaining mantle fluid migration along normal faults F1 and F2: 1) mantle fluid migration following large-scale normal faulting through the entire forearc crust; 2) migration of mantle fluids locally trapped at shallow depth.

Because a fault zone with weak coupling is prone to dilate at a seismic slip (e.g., Boulton et al., 2017), aftershocks with normal-faulting focal mechanisms, which follow the mainshock (M_w9.0), might help the normal faults (i.e., fluid conduits) to remain dilated or reactivated, allowing fluid migration along the faults from the mantle wedge. Mainshocks (i.e., "breakthrough" events) that rupture along the shallow megathrust to near the trench have greater diversity of intraplate aftershock faulting (i.e., focal mechanism and spatial distribution) than events with rupture confined to deeper portions of the megathrust (Wetzler et al., 2017). The breakthrough ruptures essentially decouple the subducting plate from the overlying plate, removing the time-varying confining regional compression and allowing activation of diverse intraplate faulting mechanisms, including outer rise normal faulting associated with plate bending stresses (e.g., Christensen and Ruff, 1988) and intraslab faulting associated with slab pull (e.g., Lay et al., 1989) and overlying plate extensional and strike-slip faulting. In fact, many normal-fault-type aftershocks were observed widely in the overlying plate and on the outer rise of the Pacific plate immediately after the 2011 Tohoku mainshock (Asano et al., 2011). These aftershocks might have been attributable to the breakthrough rupture involving shallow rupture of the 2011 Tohoku megathrust with volumetrically extensive elastic strain drop around the plate boundary that allows activation of diverse intraplate faulting (Wetzler et al., 2017). The locations of the normal faults F1 and F2 are roughly consistent with the 2011 Tohoku earthquake aftershocks, which demonstrate the normal-faulting focal mechanisms (**Figure 1**). If such a large-scale normal fault from the seafloor down to the mantle wedge were reactivated, then at least M7-class aftershocks could have occurred immediately after the 2011 M_w9.0 event. However, such a large aftershock with a normal-faulting focal

mechanism was not observed in the overlying plate (e.g., Asano et al., 2011), implying only a low probability of this case.

Alternatively, the fluid might migrate along the normal faults up to the upper part of the Cretaceous basement. Then it might be locally trapped during earlier coseismic and interseismic periods, as suggested by high-amplitude, reverse-polarity reflections (**Figure 4**) of normal faults within Unit B. The 2011 Tohoku mainshock and subsequent aftershocks can lead pre-existing normal faults to be reactive, more porous, and permeable such that the trapped fluids are easily migrated up to seafloor along the faults. Neighboring normal faults close to faults F1 and F2 can facilitate fluid migration, resulting in high ^{3}He flux and a maximum excess ^{3}He at sites N3 and N2 (Sano et al., 2014). Considering the anomalously high speed (approx. 4 km a day) of fluid migration through the entire fault conduit (Sano et al., 2014), which is much faster than that estimated from pressure-gradient propagation (e.g., Bourlange and Henry, 2007), the latter case is more likely to be accepted.

Volcanism is expected to be a major route to carry such mantle helium to Earth's surface (Sano and Fischer, 2013). In the forearc region without volcanoes, mantle wedge fluids, resulted from the dehydration reactions of the subducting Pacific slab (Zhao et al., 2015), might carry mantle-derived helium to the seafloor so that the excess ^{3}He is contained in bottom seawater (Sano et al., 2014). The slight ^{3}He/^{4}He anomaly at sites N3 and N2 revisited in 2016 (Escobar et al., 2019) suggests that the normal fault, as a fluid conduit, appears to be currently inactive and sealed. Precipitation of minerals such as calcite and phyllosilicates during the interseismic period may have sealed the fault zone (e.g., Boulton et al., 2017).

Implications of Normal Faults for Shallow Coseismic Slip

In general, normal and reverse faults can cause vertical displacement of the seafloor to push water columns upwards, eventually producing tsunami waves. Compared with tsunami waves created by thrust or reverse faults (e.g., the 2011 Tohoku earthquake and tsunami), tsunami waves by normal faults are less common in subduction zones. Nevertheless, they do occur in such places as the outer rise of the subducting plate during the 1933 Sanriku (Kanamori, 1971), 2007 Kuril (Ammon et al., 2008), and 2009 Samoa (Lay et al., 2010) earthquakes. Based on heat flow, seafloor observations, and MCS data, Tsuji et al. (2013) proposed that landward-dipping normal faults ruptured around site N1 during the 2011 Tohoku event might detach the seaward frontal crust (i.e., foot wall block) from the landward crust (i.e., hanging wall block) and then drive the foot wall block to move toward the trench (i.e., horizontal motion of the seafloor), promoting shallow coseismic slip and subsequent tsunami generation (McKenzie and Jackson, 2012). That is a similar mechanism to those occurring in the northern Japan Trench (Tanioka and Seno, 2001) and Nankai Trough (Park et al., 2010). However, there is little evidence to support that normal faults F1 and F2 ruptured entirely around sites N3 and N2 during the 2011 Tohoku event and thus generated such a horizontal motion of the seafloor. Alternatively, the potentially reactivated faults F1 and F2 may be an indicator of coseismic rupture propagation to the trench, because forearc extension is expected in the overlying plate when earthquake rupture propagates to shallow depths (e.g., Li et al., 2014; Xu et al., 2016; Bécel et al., 2017). Assuming that the ~5-m-high fault (F1) scarp observed at the seafloor on the SBP profile (**Figure 3**) is associated with large megathrust earthquakes including the 2011 Tohoku event and also develops continuously from MCS lines D6 to D13, the reactivated normal fault F1 might have produced vertical displacement of the seafloor near the fault and thus could have enhanced the local tsunami, even though this effect might be much smaller than the shallow coseismic slip. When the mantle wedge fluids enter active faults in the forearc crust, the fault-zone friction is reduced (Zhao et al., 2015). More specifically, the fluids trapped along normal faults F1 and F2, can somewhat increase the pore fluid pressure of the faults because the high-amplitude, reverse-polarity reflections are localized (**Figure 4**). Locally elevated fluid pressures might decrease the effective normal stress for the fault plane, facilitating easier slip of the fault and local tsunami generation.

Basal Erosion in the Middle Slope Region

Forearc extensional subsidence and normal faults caused by basal erosion are common in many convergent plate margins such as the Peru Trench (von Huene and Lallemand, 1990), Japan Trench (von Huene et al., 1994; Tsuru et al., 2002), and Costa Rica margin (Ranero and von Huene, 2000). Wang et al. (2011) proposed that shallow basal erosion might occur during large interplate earthquakes. Then the extension field can be formed on the forearc during interseismic wedge-stress relaxation periods. Based on seafloor observations and MCS data obtained for the Japan Trench forearc (Arai et al., 2014; Tsuji et al., 2013), those studies suggest that the episodic forearc extension and subsidence accompanied by normal faulting have occurred during coseismic events (e.g., the 2011 Tohoku earthquake). On the PSDM profile of line D6, one can identify many normal faults developing in the upper and middle slope regions. High-amplitude, reverse-polarity reflections located at a maximum of approx. 2 km above the plate interface appear to run roughly parallel to the plate interface in the middle slope region (**Figure 2B**, **Figure 7**), leading us to interpret that those reflections indicate a shear zone associated with plate subduction processes such as basal erosion. The maximum of approx. 2-km-thick material eroded from the base of overlying plate tends to thin (approx. 0.5 km) up-dip. Its down-dip extension is not clear, probably because of insufficient seismic resolution. Seismic records show a similar structure (so-called megalens) at the base of Middle America convergent margin, which suggests basal or subduction erosion (Ranero and von Huene, 2000). The high-amplitude, reverse-polarity reflections of the shear zone on the PSDM profile of line D6 suggest the presence of overpressured fluids. The base of the overlying plate is hydrofractured (e.g., von Huene et al., 2004). Consistent with potentially fluid-filled shear zone showing reverse-polarity reflections is an argument that basal erosion occurs in a low-stress environment in which fluid pressure is elevated (Le Pichon et al., 1993). Most reflections from the shear zone parallel to the plate interface appear to localize in the

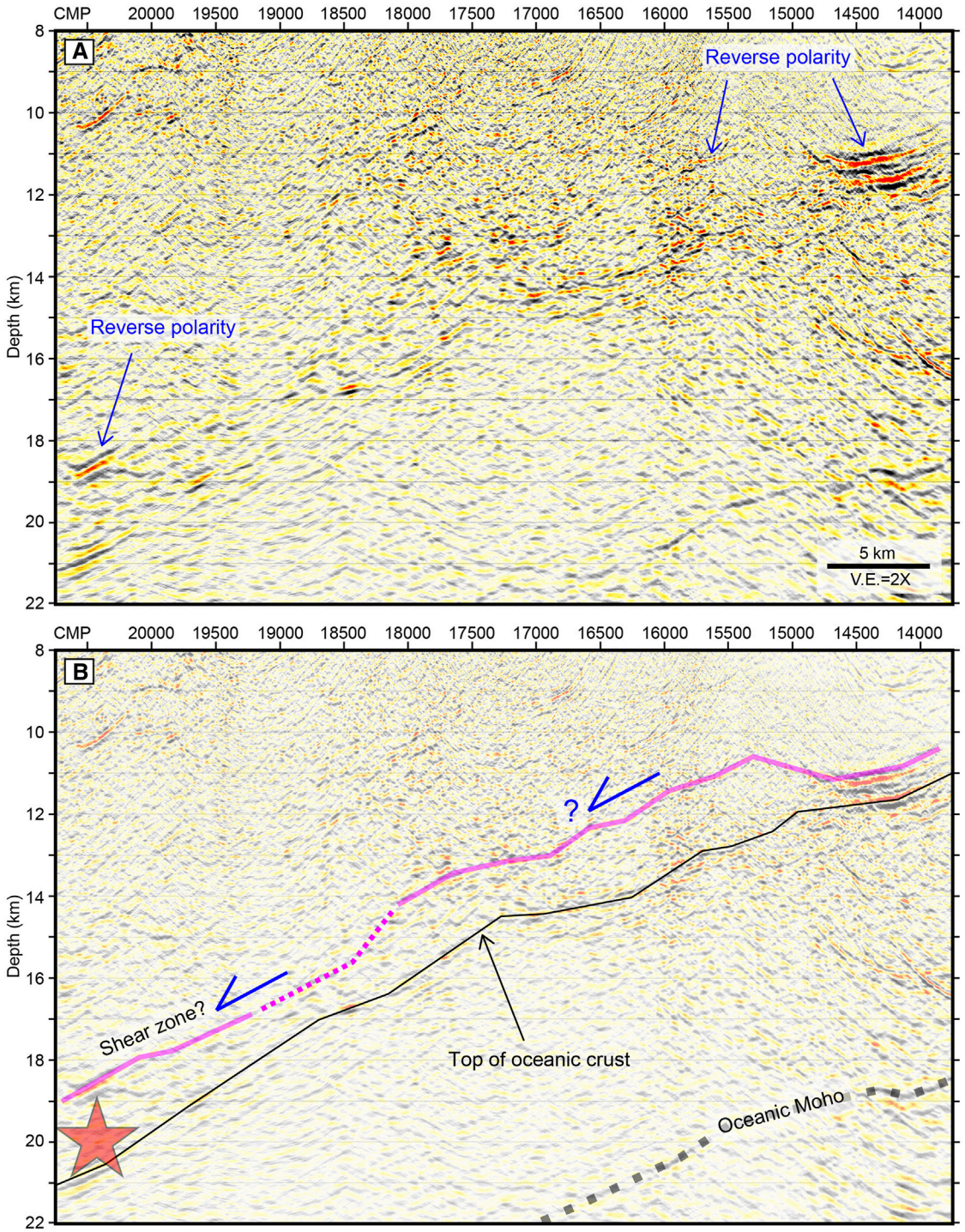

FIGURE 7 | Enlarged PSDM section on line D6 and its interpretation showing a possible shear zone in the middle slope region. The section location is presented in **Figure 2B**. **(A)** Uninterpreted PSDM section. High-amplitude, reverse-polarity reflections (black–red–black) of the shear zone (thick pink) above the top of oceanic crust. **(B)** Interpreted PSDM section. The red star marks the hypocenter of the 2011 Tohoku earthquake (M_w9.0).

middle slope region where more normal faults develop, implying more intense basal erosion in the middle slope region than in upper or lower slope regions. Kimura et al. (2012) estimated a lower interplate friction ($\mu' < 0.03$) for the middle slope region than for the upper (0.03) and lower (0.08) slope regions respectively, which shows good agreement with our inference. It is not clear whether the 2011 Tohoku earthquake was necessarily nucleated at the basal shear zone

with high-amplitude, reverse-polarity reflection (**Figure 2B**, **Figure 7**), even though its hypocenter is roughly located at the shear zone. However, fluid ovepressure in basal shear zones of the overlying plate may have favored the rupture of the 2011 Tohoku event. This hypothesis can be tested by a further investigation such as full-waveform inversion (e.g., Jamali Hondori et al., 2021) of longer-offset (>10 km) seismic reflection data, which would provide high-resolution V_p data and thus accurate pore-fluid pressures along the basal shear zone.

CONCLUSION

A) The pre-stack depth migrated profile and sub-bottom profiling data reveal landward-dipping normal faults as potential conduits for mantle-derived fluids in the coseismic slip area of the 2011 Tohoku earthquake (M_w9.0). Deep extension of the faults, characterized by high-amplitude and reverse-polarity reflections, connect to a low-velocity region spreading from the Cretaceous basement into the mantle wedge across the forearc Moho, suggesting that the faults are locally filled with mantle-derived fluids and that they are therefore potentially overpressured.

B) The 2011 Tohoku mainshock and subsequent aftershocks can lead the pre-existing normal faults to be reactive and more permeable so that the locally trapped mantle fluids can readily migrate up to the seafloor through the fracture zone of the faults.

C) The reactivated normal faults may be an indicator of shallow coseismic slip to the trench, because forearc extension is expected in the overlying plate when earthquake rupture propagates to shallow depths. Locally elevated fluid pressures can decrease the effective normal stress for the fault plane, facilitating easier slip along the fault and local tsunami.

D) We identified a possible shear zone with high-amplitude, reverse-polarity reflections above the plate interface, which is almost confined to the middle slope region, suggesting more intense basal erosion of the overlying plate in that region.

DATA AVAILABILITY STATEMENT

The original contributions presented in the study are included in the article/**Supplementary Material**, further inquiries can be directed to the corresponding author.

AUTHOR CONTRIBUTIONS

J-OP designed the study and wrote the manuscript. GF and TK conducted seismic surveys. EJH processed seismic data. TT, NT, DZ, and YS provided geological, seismological, and geochemical interpretations. All authors contributed to the final manuscript preparation.

FUNDING

This research was partially supported by a Grant-in-Aid for Scientific Research (No. 18H03732) and Earthquake and Volcano Hazards Observation and Research Program from the Ministry of Education, Culture, Sports, Science and Technology (MEXT) of Japan.

ACKNOWLEDGMENTS

We thank shipboard scientists and the crew of the R/V *Kairei* (KR11-E03) and *Shinsei-maru* (KS-16-17) cruises for their assistance in acquiring seismic reflection data. We acknowledge Y. Asano and T. Iinuma for the aftershock and coseismic slip data on the 2011 Tohoku earthquake. We also thank Paradigm/Emerson (http://www.pdgm.com) for providing seismic data processing software packages.

SUPPLEMENTARY MATERIAL

The Supplementary Material for this article can be found online at: https://www.frontiersin.org/articles/10.3389/feart.2021.687382/full#supplementary-material

REFERENCES

Ammon, C. J., Kanamori, H., and Lay, T. (2008). A Great Earthquake Doublet and Seismic Stress Transfer Cycle in the central Kuril Islands. *Nature* 451, 561–565. doi:10.1038/nature06521

Arai, K., Inoue, T., Ikehara, K., and Sasaki, T. (2014). Episodic Subsidence and Active Deformation of the Forearc Slope along the Japan Trench Near the Epicenter of the 2011 Tohoku Earthquake. *Earth Planet. Sci. Lett.* 408, 9–15. doi:10.1016/j.epsl.2014.09.048

Asano, Y., Saito, T., Ito, Y., Shiomi, K., Hirose, H., Matsumoto, T., et al. (2011). Spatial Distribution and Focal Mechanisms of Aftershocks of the 2011 off the Pacific Coast of Tohoku Earthquake. *Earth Planet. Sp* 63, 669–673. doi:10.5047/eps.2011.06.016

Bécel, A., Shillington, D. J., Delescluse, M., Nedimović, M. R., Abers, G. A., Saffer, D. M., et al. (2017). Tsunamigenic Structures in a Creeping Section of the Alaska Subduction Zone. *Nat. Geosci* 10, 609–613. doi:10.1038/ngeo2990

Boulton, C., Menzies, C. D., Toy, V. G., Townend, J., and Sutherland, R. (2017). Geochemical and Microstructural Evidence for Interseismic Changes in Fault Zone Permeability and Strength, Alpine Fault, New Zealand. *Geochem. Geophys. Geosyst.* 18, 238–265. doi:10.1002/2016gc006588

Bourlange, S., and Henry, P. (2007). Numerical Model of Fluid Pressure Solitary Wave Propagation along the Décollement of an Accretionary Wedge: Application to the Nankai Wedge. *Geofluids* 7, 323–334. doi:10.1111/j.1468-8123.2007.00181.x

Christensen, D. H., and Ruff, L. J. (1988). Seismic Coupling and Outer Rise Earthquakes. *J. Geophys. Res.* 93, 13421–13444. doi:10.1029/jb093ib11p13421

DeMets, C., Gordon, R. G., Argus, D. F., and Stein, S. (1990). Current Plate Motions. *Geophys. J. Int.* 101, 425–478. doi:10.1111/j.1365-246x.1990.tb06579.x

El Hariri, M., Abercrombie, R. E., Rowe, C. A., and Do Nascimento, A. F. (2010). The Role of Fluids in Triggering Earthquakes: Observations from Reservoir Induced Seismicity in Brazil. *Geophys. J. Int.* 181, 1566–1574. doi:10.1111/j.1365-246x.2010.04554.x

Escobar, M. T., Takahata, N., Kagoshima, T., Shirai, K., Tanaka, K., Park, J.-O., et al. (2019). Assessment of Helium Isotopes Near the Japan Trench 5 Years after the 2011 Tohoku-Oki Earthquake. *ACS Earth Space Chem.* 3, 581–587. doi:10.1021/acsearthspacechem.8b00190

Hubbert, M. K., and Rubey, W. (1959). Role of Fluid Pressure in Mechanics of Overthrust Faulting: Parts I and II. *Geol. Soc. Am. Bull.* 70, 115–205. doi:10.1130/0016-7606(1959)70[115:ROFPIM]2.0.CO;2

Ide, S., Baltay, A., and Beroza, G. C. (2011). Shallow Dynamic Overshoot and Energetic Deep Rupture in the 2011 Mw 9.0 Tohoku-Oki Earthquake. *Science* 332, 1426–1429. doi:10.1126/science.1207020

Iinuma, T., Hino, R., Kido, M., Inazu, D., Osada, Y., Ito, Y., et al. (2012). Coseismic Slip Distribution of the 2011 off the Pacific Coast of Tohoku Earthquake (M9.0) Refined by Means of Seafloor Geodetic Data. *J. Geophys. Res.* 117, a–n. doi:10.1029/2012jb009186

Jamali Hondori, E., Guo, C., Mikada, H., and Park, J.-O. (2021). Full-waveform Inversion for Imaging Faulted Structures: A Case Study from the Japan Trench Forearc Slope. *Pure Appl. Geophys.* doi:10.1007/s00024-021-02727-w

Kanamori, H. (1971). Seismological Evidence for a Lithospheric normal Faulting - the Sanriku Earthquake of 1933. *Phys. Earth Planet. Interiors* 4, 289–300. doi:10.1016/0031-9201(71)90013-6

Kimura, G., Hina, S., Hamada, Y., Kameda, J., Tsuji, T., Kinoshita, M., et al. (2012). Runaway Slip to the Trench Due to Rupture of Highly Pressurized Megathrust beneath the Middle Trench Slope: The Tsunamigenesis of the 2011 Tohoku Earthquake off the East Coast of Northern Japan. *Earth Planet. Sci. Lett.* 339-340, 32–45. doi:10.1016/j.epsl.2012.04.002

Kodaira, S., Nakamura, Y., Yamamoto, Y., Obana, K., Fujie, G., No, T., et al. (2017). Depth-varying Structural Characters in the Rupture Zone of the 2011 Tohoku-Oki Earthquake. *Geosphere* 13, 1408–1424. doi:10.1130/ges01489.1

Lay, T., Ammon, C. J., Kanamori, H., Rivera, L., Koper, K. D., and Hutko, A. R. (2010). The 2009 Samoa-Tonga Great Earthquake Triggered Doublet. *Nature* 466, 964–968. doi:10.1038/nature09214

Lay, T., Astiz, L., Kanamori, H., and Christensen, D. H. (1989). Temporal Variation of Large Intraplate Earthquakes in Coupled Subduction Zones. *Phys. Earth Planet. Interiors* 54, 258–312. doi:10.1016/0031-9201(89)90247-1

Li, S., Moreno, M., Rosenau, M., Melnick, D., and Oncken, O. (2014). Splay Fault Triggering by Great Subduction Earthquakes Inferred from Finite Element Models. *Geophys. Res. Lett.* 41, 385–391. doi:10.1002/2013gl058598

Liu, X., and Zhao, D. (2018). Upper and Lower Plate Controls on the Great 2011 Tohoku-Oki Earthquake. *Sci. Adv.* 4, eaat4396. doi:10.1126/sciadv.aat4396

McKenzie, D., and Jackson, J. (2012). Tsunami Earthquake Generation by the Release of Gravitational Potential Energy. *Earth Planet. Sci. Lett.* 345-348, 1–8. doi:10.1016/j.epsl.2012.06.036

Miura, S., Takahashi, N., Nakanishi, A., Tsuru, T., Kodaira, S., and Kaneda, Y. (2005). Structural Characteristics off Miyagi Forearc Region, the Japan Trench Seismogenic Zone, Deduced from a Wide-Angle Reflection and Refraction Study. *Tectonophysics* 407, 165–188. doi:10.1016/j.tecto.2005.08.001

Nasu, N., Huene, R. V., Ishiwada, Y., Langseth, M., Bruns, T., and Honda, E. (1980). Interpretation of Multichannel Seismic Reflection Data, Legs. 56 and 57, Japan Trench Transect, Deep Sea Drilling Project. *Initial Rep. Deep Sea Drilling Project* 56-57, 489–503. doi:10.2973/dsdp.proc.5657.112

Park, J.-O., Fujie, G., Wijerathne, L., Hori, T., Kodaira, S., Fukao, Y., et al. (2010). A Low-Velocity Zone with Weak Reflectivity along the Nankai Subduction Zone. *Geology* 38, 283–286. doi:10.1130/g30205.1

Pichon, X. L., Henry, P., and Lallemant, S. (1993). Accretion and Erosion in Subduction Zones: The Role of Fluids. *Annu. Rev. Earth Planet. Sci.* 21, 307–331. doi:10.1146/annurev.ea.21.050193.001515

Ranero, C. R., and von Huene, R. (2000). Subduction Erosion along the Middle America Convergent Margin. *Nature* 404, 748–752. doi:10.1038/35008046

Sano, Y., and Fischer, T. P. (2013). "The Analysis and Interpretation of Noble Gases in Modern Hydrothermal Systems," in *Advances in Isotope Geochemistry*. Editor P. Burnard (Berlin/Heidelberg: Springer-Verlag), 249–317. doi:10.1007/978-3-642-28836-4_10

Sano, Y., Hara, T., Takahata, N., Kawagucci, S., Honda, M., Nishio, Y., et al. (2014). Helium Anomalies Suggest a Fluid Pathway from Mantle to Trench during the 2011 Tohoku-Oki Earthquake. *Nat. Commun.* 5, 3084. doi:10.1038/ncomms4084

Tanioka, Y., and Seno, T. (2001). Sediment Effect on Tsunami Generation of the 1896 Sanriku Tsunami Earthquake. *Geophys. Res. Lett.* 28, 3389–3392. doi:10.1029/2001gl013149

Tobin, H. J., Moore, J. C., and Moore, G. F. (1994). Fluid Pressure in the Frontal Thrust of the Oregon Accretionary Prism: Experimental Constraints. *Geol* 22, 979–982. doi:10.1130/0091-7613(1994)022<0979:fpitft>2.3.co;2

Tsuji, T., Kawamura, K., Kanamatsu, T., Kasaya, T., Fujikura, K., Ito, Y., et al. (2013). Extension of continental Crust by Anelastic Deformation during the 2011 Tohoku-Oki Earthquake: The Role of Extensional Faulting in the Generation of a Great Tsunami. *Earth Planet. Sci. Lett.* 364, 44–58. doi:10.1016/j.epsl.2012.12.038

Tsuru, T., Park, J.-O., Miura, S., Kodaira, S., Kido, Y., and Hayashi, T. (2002). Along-arc Structural Variation of the Plate Boundary at the Japan Trench Margin: Implication of Interplate Coupling. *J. Geophys. Res.* 107 (B12), 2357. doi:10.1029/2001jb001664

Tsuru, T., Park, J.-O., Takahashi, N., Kodaira, S., Kido, Y., Kaneda, Y., et al. (2000). Tectonic Features of the Japan Trench Convergent Margin off Sanriku, Northeastern Japan, Revealed by Multichannel Seismic Reflection Data. *J. Geophys. Res.* 105, 16403–16413. doi:10.1029/2000jb900132

von Huene, R., Klaeschen, D., Cropp, B., and Miller, J. (1994). Tectonic Structure across the Accretionary and Erosional Parts of the Japan Trench Margin. *J. Geophys. Res.* 99, 22349–22361. doi:10.1029/94jb01198

von Huene, R., and Lallemand, S. (1990). Tectonic Erosion along the Japan and Peru Convergent Margins. *Geol. Soc. Am. Bull.* 102, 704–720. doi:10.1130/0016-7606(1990)102<0704:teatja>2.3.co;2

von Huene, R., Ranero, C. R., and Vannucchi, P. (2004). Generic Model of Subduction Erosion. *Geol* 32, 913–916. doi:10.1130/g20563.1

Wang, K., Hu, Y., von Huene, R., and Kukowski, N. (2011). Interplate Earthquakes as a Driver of Shallow Subduction Erosion. *Geology* 38, 431–434. doi:10.1130/g30597.1

Wetzler, N., Lay, T., Brodsky, E. E., and Kanamori, H. (2017). Rupture-Depth-Varying Seismicity Patterns for Major and Great (M W ≥ 7.0) Megathrust Earthquakes. *Geophys. Res. Lett.* 44, 9663–9671. doi:10.1002/2017gl074573

Xu, S., Fukuyama, E., Yue, H., and Ampuero, J. P. (2016). Simple Crack Models Explain Deformation Induced by Subduction Zone Megathrust Earthquakes. *Bull. Seismological Soc. America* 106, 2275–2289. doi:10.1785/0120160079

Yamanaka, Y., and Kikuchi, M. (2004). Asperity Map along the Subduction Zone in Northeastern Japan Inferred from Regional Seismic Data. *J. Geophys. Res.* 109, B07307. doi:10.1029/2003jb002683

Yilmaz, Ö. (2001). *Seismic Data Analysis: Processing, Inversion, and Interpretation of Seismic Data*. Tulsa, Oklahoma: Society of Exploration Geophysicists. doi:10.1190/1.9781560801580

Zhao, D., Kitagawa, H., and Toyokuni, G. (2015). A Water wall in the Tohoku Forearc Causing Large Crustal Earthquakes. *Geophys. J. Int.* 200, 149–172. doi:10.1093/gji/ggu381

Conflict of Interest: The authors declare that the research was conducted in the absence of any commercial or financial relationships that could be construed as a potential conflict of interest.